# Thermal Decomposition Kinetics of a Synthetic K-$H_3O$ Jarosite Analog

Keywords: K-$H_3O$ Jarosite, Thermal decomposition, Kinetics, Isoconversion, Reaction mechanism

TA375

## ABSTRACT

Thermal decomposition of a synthetic K-$H_3O$ jarosite analog was investigated. A complex reaction model describing the decomposition sequence was proposed based on features observed from thermogravimetic analysis and X-ray diffraction analysis of partially decomposed jarosite. Observed $(OH)^-$ and $SO_3$ loss was broken down into subreactions. Kinetic data was determined by isoconversion analysis to describe the individual subreactions. The predicted model reasonably matched the observed decomposition. The results pertaining to the identification of subreactions and assignment of kinetic triplet data described in this paper will be the basis for potential use of jarosite type minerals as thermal witness materials.

## INTRODUCTION

Jarosites are complex sulfate hydrates that belong to the alunite super group. They are minerals commonly found in the weathering zones near sulfide ore deposits and a common byproduct of mining operations[1, 2]. Jarosites undergo decomposition upon heating. The decomposition occurs as a series of well-distinguished steps, where adsorbed water, $(OH)^-$ groups, and $(SO_4)^{2-}$ groups are lost sequentially. Jarosite, in the strict sense, ceases to exist after the loss of $(OH)^-$ groups. The thermal decomposition of jarosite and other members of the alunite super group have been studied previously. Various analytical techniques such as thermogravimetric analysis (TGA), X-ray diffraction spectroscopy (XRD), Nuclear magnetic resonance (NMR) have been employed to study the thermal decomposition and structure of these minerals. A number of reactions describing the decomposition sequence [3, 4] and its structural implications has been published [5].

The present study examines the thermal decomposition of a synthetic K-$H_3O$ jarosite analog and attempts to develop a comprehensive decomposition model by identifying the relevant intermediate reaction steps, and quantifying kinetic relations.

## EXPERIMENTAL

K-$H_3O$ jarosite was synthesized following a procedure published previously [6, 7]. X-ray diffraction and electron microscopy were used to characterize the material's exact composition and homogeneity [8].

Thermo-gravimetric analysis (TG) was used to characterize thermal decomposition, and to develop a quantitative decomposition model. A TA Instruments model Q5000IR thermo-gravimetric analyzer with alumina sample pans was used. The balance was purged with argon (Matheson Tri-Gas, 99.999%) at 10 ml/min and the furnace was purged with air (Airgas, zero grade) at 25 ml/min. Sample masses were ~1 mg; baseline corrections became significant. Therefore, each sample was heated twice without removing the sample from the TG. The actual decomposition was recorded during the first cycle, and the baseline during the second cycle. The second heating signal was subtracted from the first heating signal, yielding the actual decomposition curve. Decomposition was studied at constant heating rates, ranging from 5 to 50 K/min, at constant reaction rates of 0.05, 0.1, 0.2 and 0.4 wt.-%/min, and using modulated TGA (MTGA) at 5 K/min with a modulation amplitude of ±10K and period of 120s.

## RESULTS

Typical decomposition behavior of jarosite is shown in figure 1. The top part of the curve was recorded at constant heating rate of 5 K/min and the bottom curve at constant mass loss rate of 0.05 wt%/min. The decomposition occurs in a stage wise manner as reported earlier [3, 4, 7]. The first stage is attributed to the loss of absorbed water, followed by the loss of $(OH)^-$ groups in the form of water and finally the loss of $(SO_4)^{2-}$ groups in the form of $SO_3$. The $SO_3$ loss stage shows some internal structure, suggesting several interacting decomposition reactions. A better resolution of the $SO_3$ loss structure is observed in the constant reaction rate experiments (figure 1).

The overall decomposition behavior of the material was investigated by recovering samples heated at 5K/min to 528 K, 710 K and 1073 K, to obtain partial decomposition products for XRD analysis. Additionally, material was also recovered from the constant-reaction rate experiment at 839 K. The jarosite XRD pattern for the sample recovered from 528 K, after the adsorbed water loss is identical to that of the initial material. It is likely that this water is loosely bonded to the surface, or resides within the pores. The sample recovered from 710 K, after the OH loss, is largely amorphous. Weak peaks of $Fe(SO_4)(OH)$, $KFe(SO_4)_2$, and of β-$Fe_2O_3$ are visible. The material recovered from the constant-reaction-rate experiment at 839 K is also poorly crystalline, and contains some amount of β-$Fe_2O_3$ and $K_3Fe(SO_4)_3$ (identified using reference 30-0943, PDF-4+ Database, ICDD 2010). The final decomposition product, recovered from 1073 K shows expected α-$Fe_2O_3$ and $K_2SO_4$ as crystalline phases.

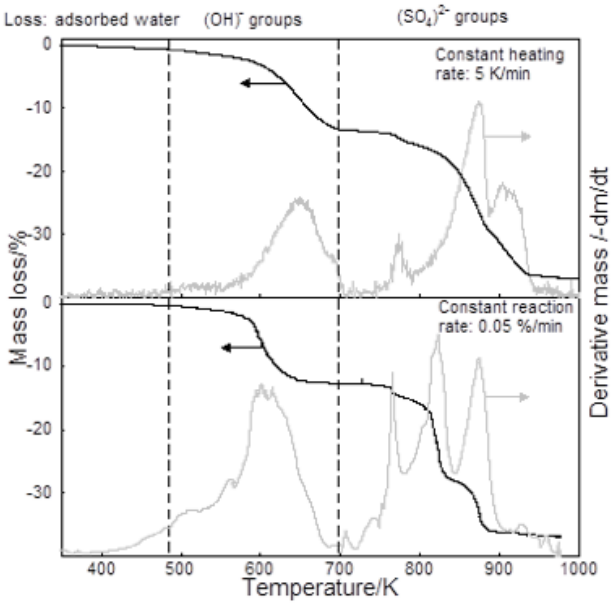


*Figure 1: Mass loss and derivative mass loss of jarosite heated at 5 K/min and under constant-reaction rate conditions.*

To determine the kinetics of decomposition, experiments were performed over a range of heating rates. For the decomposition model, Arrhenius kinetics where assumed to be valid, so that the reaction rate can be described as

$$d\alpha/dt = k(T)\cdot f(\alpha) = A\cdot\exp(-E_A/RT)\cdot f(\alpha) \quad (1)$$

where α represents a suitably defined reaction progress function, A is the pre-exponential factor of this reaction, and $E_A$ the corresponding activation energy. The reaction model is given as f(α).

Activation energies were determined as a function of global reaction progress using an isoconversion method as stated in [6]. The overall reaction progress was defined as $\alpha = (m - m_0)/(m_f - m_0)$ with $m_0$ and $m_f$ as the initial and final masses, respectively. Because at constant reaction progress, the reaction rate should only depend on the temperature, measurements at different heating rates can be compared in order to obtain activation energies for that reaction progress. The particular algorithm of the isoconversion approach used here uses the function J:

$$J[E_\alpha, T_i(t_\alpha)] = \int_{t_{\alpha-\Delta\alpha}}^{t_\alpha} \exp\left[\frac{-E_\alpha}{RT_i(t)}\right]dt \quad (2)$$

which is calculated for each heating program $T_i(t)$ over the time interval $t_\alpha$-$t_{\alpha-\Delta\alpha}$ corresponding to an interval Δα. The activation energy $E_\alpha$ is adjusted so that the differences between measurements with different heating programs are minimized. Systematic application of this algorithm over the whole complex decomposition gives the overall apparent activation energy for a set of values of α. The algorithm was implemented in MATLAB; reference [6] has more details.

Activation energies were also calculated from modulated TGA experiments following the procedure published in [9]. Due to the temperature modulation, the temperature-time record has a series of peaks (subscript p) and valleys (subscript v). With the assumption that the reaction mechanism shows negligible change between a peak $T_p(t)$ and the adjacent valley $T_v(t)$, the following equation can be used to estimate the activation energy of the corresponding interval $\alpha_v$-$\alpha_p$:

$$E_{\alpha_v,\alpha_p} = \frac{RT_vT_p\ln(d\alpha_v/d\alpha_p)}{T_v - T_p} \quad (3)$$

where $d\alpha_v/d\alpha_p$ is the ratio of the reaction rates, dα/dt for the peak-valley pair.

All estimates for the activation energy as function of the global reaction progress are shown in figure 2. Despite minor variation between the different methods (constant HR, constant reaction rate, MTGA), the results are consistent; further details are discussed for the constant heating rate results.

Several regions in the α curve with relatively constant apparent activation energies can be identified. The divergent behavior seen at $\alpha \to 0$, $\alpha \approx 0.35$, and $\alpha \to 1$ is commonly observed in regions were the reaction progress α changes very little. The range α = 0.05 – 0.35, observed between 600 and 700 K in figure 1, and attributed to the loss of $(OH)^-$ shows an average apparent activation energy of 160 kJ/mol. At the end of this step, near α = 0.35, a short interval with a higher activation energy approaching 300 kJ/mol, can be identified in figure 2.

Following this, a small step near 800 K can be identified in figure 1; it is more distinct at constant reaction rate conditions. The following interval α = 0.45 – 0.75, 800 – 850 K in figure 1, shows a relatively constant average apparent activation energy of 225 kJ/mol with constant heating rate. This interval transitions to a region with an apparent activation energy of 350 kJ/mol around α = 0.8, and the decomposition ends with an interval between α = 0.86 – 0.97 with an apparent activation energy of 180 kJ/mol.

The analysis of the partial decomposition products, together with data from the literature was used to formulate a complex model for the entire decomposition process, shown schematically in figure 3 [3]. The intermediate species identified by X-Ray diffraction are highlighted in figure 3.

To calculate net decomposition curves according to the model shown in figure 3, each reaction appearing as an arrow in figure 3, was assigned a "kinetic triplet": activation energy, pre-exponential factor, and reaction model. Starting with the original, undecomposed material, the formation and decomposition of each subsequent product was tracked. This allowed the definition of a reaction progress $\alpha_i$ for each individual reaction in figure 3. From the individual product amounts, the overall reaction progress was calculated by summing up the masses of all products present at any point of time in the heating program. This algorithm was implemented in MATLAB in order to compute the decomposition. Where possible, activation energies were taken from the isoconversion analysis (figure 2). Some reactions, e.g. the loss of $H_3O^+$, contributed only minorly to the overall mass loss, therefore could not be resolved, and were lumped together with respective parallel reactions. For the models, first-order reactions were assumed as default;

only where a satisfactory match between experiment and computation could not be achieved, were other models used. Pre-exponential factors were varied to achieve a match between experiment and computation. The process of derivation of the model – necessarily abbreviated here – is elaborated rigorously in ref [8].

The kinetic parameters are shown in Table 1, and computed decomposition curves are shown in figure 4. Experimental and calculated curves are close over the entire temperature range; the effect of heating rate is also well reproduced.

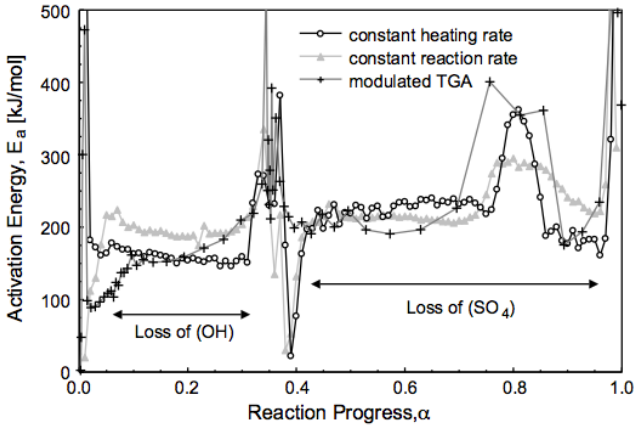


*Figure 2: Apparent activation energies determined by isoconversion analysis, and from MTGA experiments.*

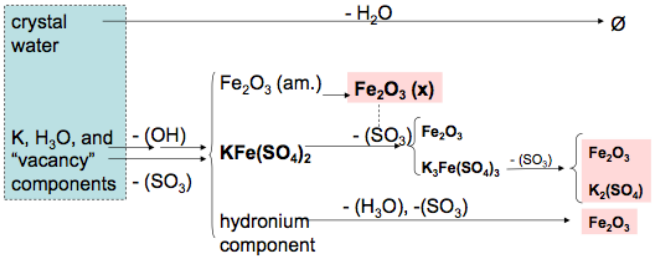


*Figure 3: Reaction scheme of jarosite thermal decomposition, intermediate species identified from XRD are highlighted in bold.*

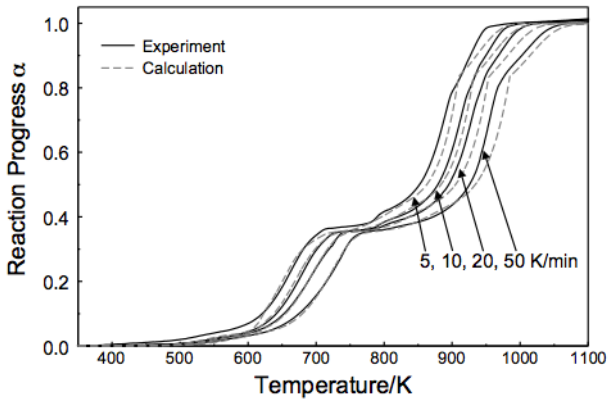


*Figure 4: Comparison between observed and calculated decomposition of K-jarosite.*

## CONCLUSION

A complex decomposition model of synthetic K-$H_3O$ jarosite was established via results compiled from TGA experiments and X-ray analysis. Activation energy was evaluated by independent techniques. A complex decomposition model was derived incorporating sequential and parallel reactions of different intermediate species that are described by constant kinetic triplets. Despite the simplifications the model describes the observed decomposition reasonably well and is also consistent with the previously reported decomposition behavior of K-jarosite. The results shown here provide the basis for potential use of jarosite group materials as thermal witness materials [8, 10].


## ACKNOWLEDGEMENT

This work was contributed by Shashank Vummidi Lakshman as part of the TA Instruments Student Applications Award Program.


*Table 1: Kinetic parameters used in the reaction scheme shown in figure 4.*

| | Associated mass loss in units of global α | Activation energy / kJ/mol | Pre-exponential factor / log(A) | Reaction model |
|---|---|---|---|---|
| Loss of adsorbed water | 0.034 | 150 | 11 | 3-D diffusion |
| Loss of $(OH)^-$, first step carrying no mass loss | – | 250 | 18.2 | first order |
| Loss of $(OH)^-$, second step | 0.287 | 125 | 7.5 | first order |
| $SO_3$ loss from the "vacancy component" | 0.019 | lumped with $(OH)^-$ loss | | |
| Crystallization of $Fe_2O_3$ carrying no mass loss | – | 525 | 33 | first order |
| Loss of $SO_3$ from $KFe(SO_4)_2$ | 0.400 | 215 | $9.5 + 0.85(1 - \alpha_{Fe2O3\text{-}cryst})$ | zero order |
| $SO_3$ loss from the hydronium component | 0.059 | lumped with previous step | | |
| Loss of $SO_3$ from $K_3Fe(SO_4)_3$ | 0.200 | 220 | 9.5 | first order |

**REFERENCES**


1. J. E. Dutrizac and J. L. Jambor, Reviews in Mineralogy and Geochemistry, 2000. 40(1): p. 405-452

2. R. E. Stoffregen, C. N. Alpers and J. L. Jambor, Alunite-jarosite crystallography, thermodynamics, and geochronology, 2000. 40: p. 453-479

3. R. L. Frost, M. L. Weier and W. Martens, Journal of Thermal Analysis and Calorimetry, 2005. 82(1): p. 115-118

4. R. L. Frost, R. A. Wills, J.T. Kloprogge and W. N. Martens, Journal of Thermal Analysis and Calorimetry, 2006. 83(1): p. 213-218

5. H. Xu, Y. Zhao, S. Vogel, D. Hickmott, L. Daemen and M. Hartl, Physics and Chemistry of Minerals, 2010. 37(2): p. 73-82

6. P. B. Gerald, S.S. Earl and A. Richard, The American Mineralogist, 1962. 47(1 ): p. 112-126

7. C. Drouet and A. Navrotsky, Geochimica et Cosmochimica Acta, 2003. 67(11): p. 2063-2076

8. S. Vummidi Lakshman, S. Mohan, E.L. Dreizin and M. Schoenitz, Journal of Thermal Analysis and Calorimetry, 2013: p. 1-12

9. R.L. Blaine and B. K. Hahn, Journal of Thermal Analysis and Calorimetry, 1998. 54(2): p. 695-704

10. S. Vummidi Lakshman, Dreizin, E., Schoenitz, M.,Journal of Thermal Analysis and Calorimetry, (submitted)


For more information or to place an order, go to http://www.tainstruments.com/ to locate your local sales office information.